The Plant Journal (1996) **10**(4), 745–754

TECHNICAL ADVANCE

Fluorescent imaging of GUS activity and RT-PCR analysis of gene expression in the shoot apical meristem

Andrew J. Fleming[1], Thianda Manzara[2,†], Wilhelm Gruissem[2] and Cris Kuhlemeier[1,*]
[1]*Institute of Plant Physiology, University of Berne, Altenbergrain 21, CH-3013 Bern, Switzerland, and*
[2]*Department of Plant Biology, University of California, Berkeley, CA 94720, USA*

Summary

The use of promoter–reporter gene constructs in transgenic plants is a powerful tool in the analysis of gene expression which can, however, be limited in the resolution of small structures, such as the apical meristem. This paper reports on a fluorescent imaging technique for the analysis of GUS reporter gene expression to cellular resolution in the apical meristem of tomato. Using this technique in combination with an RT-PCR analysis of *RBS* gene-specific transcript levels, it is shown that: 5′ upstream sequences of *RBCS* genes are sufficient to mimic the pattern of transcripts revealed by *in situ* hybridisation (no expression in the apical meristem, high expression in the initiated leaf primordia); the genes *RBCS2, RBCS3A* and *RBCS3B* are transcriptionally activated upon primordium initiation with transcripts for *RBCS1* and *RBCS3C* accumulating later in leaf development; and that *RBCS* promoter activity cannot be induced in the apical meristem by light, an environmental signal which elevates *RBCS* transcript level in other aerial parts of the plant. These data provide a detailed picture of the complex transcriptional events occurring on leaf initiation and the establishment of the photosynthetic machinery; they describe two complementary techniques which allow the analysis of such complex events at the tissue and cellular level; and they characterize an *in vivo* assay system which can be used to analyse the factors involved in the initiation and maintenance of gene expression patterns in the apical meristem.

Introduction

Our previous work has shown that genes are expressed in the vegetative apical meristem in a number of distinct patterns (Fleming and Kuhlemeier, 1994; Fleming *et al.*, 1992, 1993). One of the most striking of these patterns was that shown by the transcripts for the small subunit of Rubisco (*RBCS*) which are not detectable within the meristem, but which accumulate in differentiating leaf and stem tissue immediately proximal to the meristem. In order to analyse the regulatory elements involved in the generation of this pattern, we decided to examine reporter gene (GUS) expression in transgenic plants under the control of *RBCS* promoter sequences (Meier *et al.*, 1995). However, this analysis of promoter–GUS construct expression in the region of the meristem posed two technical problems. First, the standard histochemical analysis of GUS activity did not provide sufficient spatial resolution in the small meristem tissue samples. We therefore developed a confocal scanning laser microscope imaging method for the visualization of GUS activity in small tissue samples. This approach provided both a high-resolution analysis of GUS activity, and also involved relatively little tissue invasion, in contrast to the destructive standard GUS histochemical approach. A second problem that we faced was that *RBCS* in tomato is encoded by a small gene family and from our *in situ* hybridization analysis it was impossible to assess whether the transcript accumulation observed outside of the meristem was due to the expression of all five *RBCS* genes present in tomato or only a subset. Owing to the small tissue samples involved (leaf primordia), classical analysis by RNA blot hybridization using gene-specific probes would have required extensive and tedious tissue dissection and collection. We therefore developed an RT-PCR analysis which provided us with data on the time-dependent accumulation of specific *RBCS* transcripts during leaf primordium development. This allowed us to identify the genes whose expression is associated with the earliest events of leaf differentiation.

We thus report here on a combined approach of fluorescent imaging of GUS reporter gene expression and RT-PCR analysis which has allowed us to create a high spatial resolution *in vivo* assay with which we can start to analyse the regulation of *RBCS* gene expression in the meristem. Using this system, we show that *RBCS* expression in the meristem cannot be induced by light.

Results

Visualization of RBCS-*GUS reporter gene acivity by fluorescent imaging*

Although the standard histochemical assay for GUS activity has many advantages in terms of speed and simplicity

Received 4 March 1996; revised 10 June 1996; accepted 18 July 1996.
*For correspondence (fax +41 31 332 2059;
e-mail kuhlemeier@pfp.unibe.ch).

(Jefferson *et al.*, 1987), our initial experiments suggested that it lacked sufficient resolution for the analysis of reporter gene activity in the apical meristem. We therefore investigated alternative methods for the visualization of GUS activity in small tissue samples. The results of this investigation, in which we used tomato leaf tissue transgenic for an *RBCS3A*–GUS construct (Meier *et al.*, 1995) as a ready source of plant material, are shown in Figure 1.

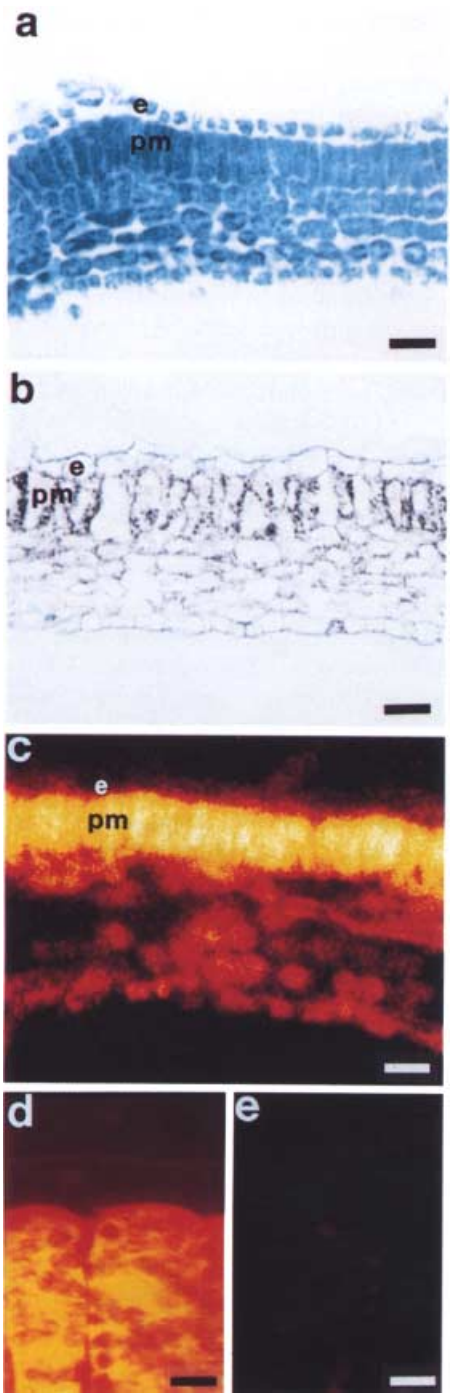

Figure 1. See legend on facing page.

An alternative to direct visualization of the blue indole X-Gluc product in fresh tissue is to embed the tissue in a matrix which allows thin sections to be cut. As shown in

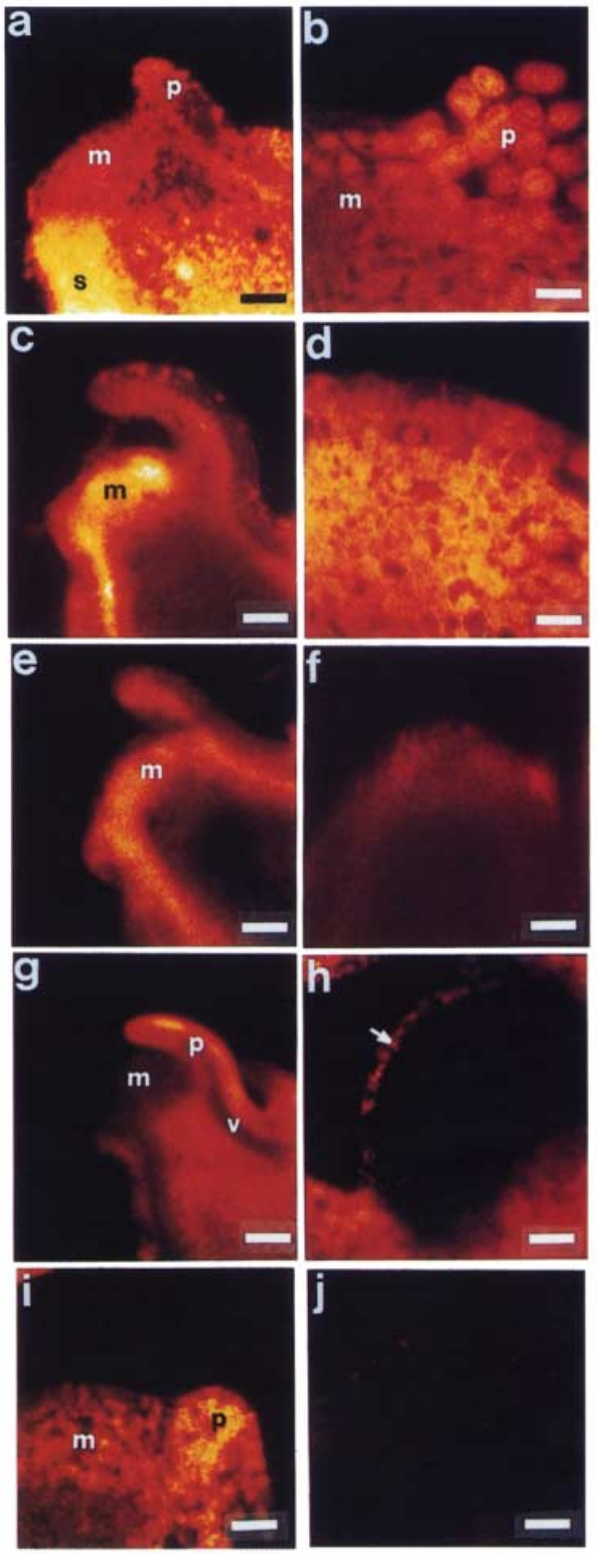

Figure 2. See legend on facing page.

Figure 1(a), this analysis leads to a good cellular resolution. However, this approach also leads to an increased processing time for each sample (4–5 days) and, moreover, the long incubation times required to produce the strong blue colour necessary for signal visualization in thin sections can lead to problems of product diffusion. For example, in Figure 1(a) a definite GUS signal is visible in the leaf epidermis, a tissue in which the *RBCS* promoter is expected to be generally inactive (Aoyagi *et al.*, 1988). The epidermis is adjacent to cells of the palisade mesophyll layer in which a very high activity of the *RBCS* promoter is to be expected.

Instead of visualizing GUS enzyme activity, we attempted to localize the GUS protein by immunocytochemistry in thin sections, as shown in Figure 1(b). This approach led to a good cellular resolution, and, in some cases, a good signal-to-noise ratio. Moreover, this approach avoided the potential diffusion problems of the histochemical approach, and led to the visualization of a very high signal in the mesophyll cells and a very low signal in the epidermal cell layer, as expected from the published data. However, the immunocytochemical approach involved a long processing time per sample (4–5 days), some technical expertise, and, most importantly, in our hands proved difficult to use as a reproducible technique. This variability in signal-to-noise ratio limited its feasibilty for the routine analysis of samples.

Confocal laser scanning microscopy (CFLS) provides a technique for high-resolution visualization of fluorescent signals from diffuse sources, and membrane permeable substrates for the GUS enzyme which release a fluorescent product on hydrolysis have become commercially available (ImaGene Green, Molecular Probes). We therefore investigated the utility of fluorescent imaging of GUS enzyme activity in thin hand sections of leaf incubated with the ImaGene Green substrate. As shown in Figure 1(c), this method of analysis provided a relatively good cellular resolution. Moreover, there is little evidence for product diffusion, a very high fluorescent signal being visible in the palisade cells adjacent to epidermal cells showing only background fluorescence, as shown in the optical section in Figure 1(d). Comparison with wild-type (non-transgenic tissue) processed in parallel with the ImaGene Green substrate (Figure 1e) indicates that the signal observed in the transgenic tissue reflects GUS activity.

Figure 1. Visualization of GUS activity by fluorescent imaging.
(a) Visualization by X-Gluc. Leaves transgenic for *RBCS*-GUS were incubated in the histogenic substrate X-Gluc before embedding and cutting of 10 μm sections. Signal is seen as a blue precipitate. Bar is 100 μm.
(b) Visualization by immunocytochemistry. Sections (10 μm) of leaf tissue transgenic for *RBCS*-GUS were incubated with an anti-GUS antibody before visualization by silver enhanced gold immunolabelling. Signal is visible as a dark brown/black precipitate. Bar is 100 μm.
(c) Visualization by fluorescent imaging. Thin hand sections of leaf tissue transgenic for *RBCS*-GUS were incubated in ImaGene Green before visualization by fluorescence microscopy. Signal has been converted to a glowscale in which white/yellow represents relatively high signal, red relatively low signal, and black zero signal. Bar is 100 μm.
(d) Confocal image of a portion of the sample shown in (c) at the interface of the palisade and epidermal layers. Signal has been converted into a glowscale as described in (c). Bar is 10 μm.
(e) Confocal image of the interface of the palisade and epidermal layers in wild-type leaf tissue hand section incubated with the ImaGene Green substrate and then visualized using essentially the same confocal parameters as used in (d). Bar is 10 μm.
Abbreviations: e, epidermis; pm, palisade mesophyll.

Figure 2. Fluorescent Imaging of *RBCS* promoter activity in the apex.
(a) Fluorescent image of an apex transgenic for *RBCS3A*-GUS. A dissected apex was incubated with the ImaGene Green substrate and signal converted into a glowscale as described in Figure 1(c). Bar is 50 μm.
(b) Confocal image of an area of an apex transgenic for *RBCS3A*-GUS. The sample was prepared as described in (a). Bar is 10 μm.
(c) Fluorescent image of an apex transgenic for 35S-GUS. A dissected apex was prepared as described in (a). Bar is 60 μm.
(d) Confocal image of an area of the meristem dome shown in (c). Bar is 10 μm.
(e) Fluorescent image of an apex incubated with acridine orange. A hand dissected wild-type apex was incubated in acridine orange before visualization by fluorescent imaging. Signal has been converted into a glowscale, as described in Figure 1(c). Bar is 60 μm.
(f) Fluorescent image of a wild-type apex prepared and incubated in the ImaGene Green substrate as described in (a). The image has been visualized using essentially the same parameters as used in (a). Bar is 60 μm.
(g) Chlorophyll autofluoresence of a wild-type apex. Signal has been converted to a glowscale as described in Figure 1(c). Bar is 80 μm.
(h) Chlorophyll autofluorescence in a wild-type meristem. Signal has been converted to a glowscale as described in Figure 1(c). The arrow points to the LI layer of the meristem dome. Bar is 20 μm.
(i) Confocal image of an apex transgenic for *RBCS3A*-GUS which has been dissected to expose the apical meristem then cultured under light for 5 days. The newly arisen primordia have been cut back before incubation of the apex with the ImaGene Green substrate. Signal has been converted into a glowscale as described in Figure 1(c). Bar = 50 μm.
(j) Confocal image of a wild-type apex prepared and incubated in parallel with that described in (i) and visualized using essentially the same parameters. Bar is 50 μm.
Abbreviations: m, meristem; p, primordium; s, stem; v, vascular tissue.

Analysis of RBCS*–GUS activity in the shoot apex*

Based on our characterization of reporter gene visualization techniques, we proceeded to analyse the pattern of *RBCS* promoter activity in the region of the apical meristem using fluorescent imaging of GUS activity. The results of this analysis are shown in Figure 2. The promoter–GUS constructs used were sufficient to reconstruct an expression pattern in the shoot apex similar to that shown for *RBCS* transcript accumulation in wild-type plants by *in situ* hybridization analysis (Fleming *et al.*, 1993). As shown in Figure 2(a), low GUS activity was observed in the meristem and high activity in the developing leaf and subtending stem tissue. A sharp boundary was observed between expressing and non-expressing cells early in leaf development, as shown by the optical section at the edge of the meristem dome and forming primordium in Figure 2(b). A gradient of reporter gene activity was generally visible

Table 1. Stages of leaf primordium development

Stage	Morphology	Length	Chlorophyll	Anthocyanin
P1	Peg	<200 μm	Colourless	Absent
P2	Peg	0.2–0.4 mm	Faint green	Absent
P3	Lobes visible	0.4–0.8 mm	Green	Faint
P4	Lobed	0.8–2 mm	Green	Present

along the axis of young primordia, with the highest signal being apparent at the tip of the primordia. No significant signal was visible in epidermal cells, except in occasional spots, probably corresponding to guard cells.

All the transgenes analysed showed no expression of the GUS enzyme in the meristem and high expression in leaf tissue. The boundary at which promoter activity first became detectable depended both on the construct and the expression level of the individual transgene. This made a judgement of differences in the spatial expression of the five different *RBCS* constructs analysed difficult.

As a control for the observed non-expression of *RBCS* constructs in the apical meristem, we analysed a number of tomato plants transgenic for a 35S–GUS construct. Our analysis of total fluorescence revealed a high level of GUS activity throughout the apical meristem, but there seemed to be a layer toward the outside of the dome in which there was a relatively low level of signal (Figure 2c). Confocal imaging also revealed that there was a non-uniform expression pattern within the meristem, as shown in Figure 2(d).

However, when apices of wild-type plants were stained with acridine orange (a general stain for nucleic acids) and the fluorescent image visualized, a similar pattern to that observed for 35S–GUS activity was recorded, that is, a relatively high signal was recorded in the inner tissue of the apical meristem (Figure 2e). Controls performed using wild-type apices incubated with the ImaGene Green substrate indicated that the signals observed in the transgenic plants reflected GUS activity (Figure 2f).

As a further control for the reliability of the data obtained using the fluorescent imaging technique, we also visualized the distribution of chlorophyll autofluorescence in the apex. As shown in Figure 2(g), chlorophyll fluorescence is apparent in the developing leaf primordia and stem tissue subtending the meristem, but appears to be absent from the meristem and vascular tissue. However, at higher magnification it is apparent that in the outermost layer of the meristem (LI) a weak fluorescence is visible (Figure 2h). In the inner bulk of the meristem dome, fluorescence is totally absent, with a sharp transition occurring between fluorescent and non-fluorescent tissue.

Previous investigations have shown that *RBCS* transcription is regulated by light in leaf and hypocotyl tissue (Kuhlemeier *et al.*, 1988; Neuhaus *et al.*, 1993). We therefore investigated whether the non-expression of the *RBCS*–GUS constructs in the meristem was due to a problem of light accessibility, since the meristem is enclosed within the expanding leaf primordia. We dissected transgenic apices containing *RBCS*–GUS constructs to reveal the apical meristem and cultured them under light for periods of up to 7 days. Fluorescent analysis of GUS expression in the region of the apex revealed a pattern of activity very similar to that observed in non-dissected tissue, that is, no expression in the meristem (Figure 2i). Dissected wild-type apices cultured and visualized under the same conditions showed only low background fluorescence (Figure 2j).

RT-PCR analysis reveals differential accumulation of RBCS *transcripts during the earliest stages of primordium development*

As described in the previous section, the plant-to-plant variability in transgene expression for the five *RBCS*–GUS constructs analysed made it very difficult to discriminate differences in the level of promoter activity using fluorescent imaging of GUS activity. With the aim of identifying which *RBCS* genes were associated with the highest transcript levels at the earliest stage of leaf development, we developed a semi-quantitative RT-PCR analysis of gene-specific *RBCS* transcript levels. This strategy required the dissection of tomato apices and assigning a developmental stage to each leaf primordium collected. The apical meristem is surrounded by a concentric series of leaves which form a spiral around the meristem. If the youngest primordium being formed is termed P1, then each successively older primordium can be designated P2, P3, P4, etc., in a developmental gradient. In plants of different absolute age, primordia of the same P number show similar developmental phenotypes, as summarized in Table 1. Although dissection of the youngest primordium, P1, from the meristem is possible, it is not facile, therefore in this study both the meristem and P1 were collected together intact and designated M+P1. RNA extracted from these samples was used in an RT-PCR analysis to examine the changes in relative level of specific *RBCS* transcripts during the earliest stages of leaf development.

To provide an internal control for the small amounts of mRNA substrate in different RT-PCR reactions, we analysed the M+P1, P2, P3 and P4 samples using primers for a

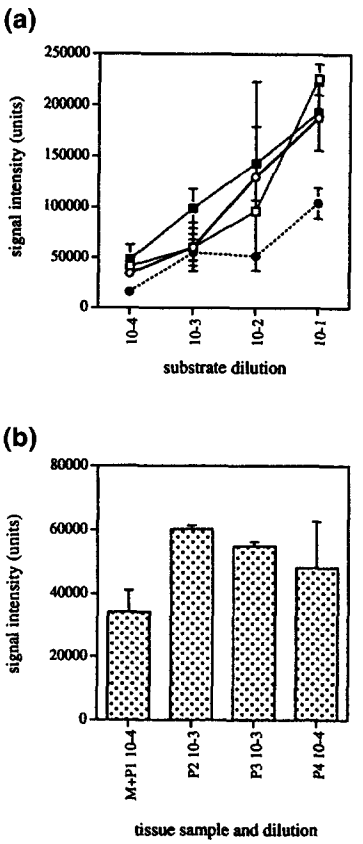

Figure 3. RT-PCR analysis of ribosomal protein mRNA, *RPL2*.
(a) Dilution curves for substrates extracted from (○) M+P1, (□) P2, (●) P3 and (■) P4 tissue samples. Each sample was amplified using a primer pair specific for *RPL2*, as described in Table 2 (error bars are standard deviation, n = 4).
(b) Bar chart showing the approximately equivalent *RPL2* signal obtained following amplification of samples M+P1 and P4 at 10^{-4} dilution, and samples P2 and P3 at 10^{-3} dilution (error bars are standard deviation, n = 4).

constitutively expressed ribosomal protein transcript, *RPL2* (see Experimental procedures and Fleming *et al.*, 1993). The results of this analysis are shown in Figure 3. They indicate, first, that the RT-PCR analysis was in the linear range for each sample (Figure 3a). Secondly, the bar chart in Figure 3b shows that the 10^{-4} substrate dilutions of samples M+P1 and P4, and the 10^{-3} substrate dilutions of samples P2 and P3 gave rise to similar (within a twofold range) *RPL2* signals after substrate amplification and thus contained similar concentrations of the *RPL2* mRNA.

The results of four independent experiments analysing RBCS gene-specific transcript levels during leaf development are shown as bar charts in Figure 4(a)–(e). They have been expressed relative to the signal obtained using the *RPL2* primers at the corresponding sample dilutions. At these sample dilutions the amplifications were in a linear range (data not shown), and autoradiographs of typical samples from which the data in the bar charts were obtained are shown in Figures 4(f)–(j).

In sample tissue at the M+P1 stage, transcripts for *RBCS2, RBCS3A,* and *RBCS3B* are present, whereas transcripts for *RBCS1* and *RBCS3C* are not detectable (Figure 4a and f). The average signal intensity observed for *RBCS2* is significantly higher than that for *RBCS3A* and *RBCS3B,* and this pattern is maintained during the developmental stages P2 and P3, although in P3 samples signals with primers for *RBCS1* and *RBCS3C* were occasionally detectable (Figure 4b and g, and c and h). In RNA extracted from P4 tissue, transcripts corresponding to *RBCS1* and *RBCS3C* were consistently detected, albeit at a relatively low level compared with *RBCS2, RBCS3A* and *RBCS3B* (Figure 4d and 4i). In young leaf tissue (developmental stage P7, P8), all five *RBCS* transcripts are readily detectable (Figure 4e and j).

To verify that the RT-PCR anaysis would have detected any major changes in relative *RBCS* transcript level during the stages of primordium development examined, we performed an analysis of etiolated and greening (etiolated + 1 day light) cotyledons of tomato seedlings. The results of the RT-PCR analysis (not shown) indicated that in tissue extracted from etiolated cotyledons, transcripts for *RBCS2* and *RBCS3A* predominated and those for *RBCS1, RBCS3B* and *RBCS3C* were barely detectable. After 24 h illumination, transcripts for all five *RBCS* transcripts were detectable and those for *RBCS3B* and *RBCS3C* represented a significant contribution to the total pool of *RBCS* RNA. These results are essentially similar to previous data obtained by RNA slot blot analysis which showed that in etiolated cotyledons the transcripts for *RBCS3B* and *RBCS3C* are not detectable, whereas all five *RBCS* transcripts are present in greening cotyledons (Wanner and Gruissem, 1991).

Discussion

In this paper, we report a high-resolution analysis of *RBCS* expression in the region of the apical meristem which allows us to identify in which cells *RBCS* genes become transcriptionally active, and which genes are responsible for the most rapid accumulation of *RBCS* transcripts. These data, in conjunction with the availability of a number of transgenes containing *RBCS* promoter–GUS constructs, allow us to use the RBCS genes as markers to analyse the factors involved in the regulation of gene expression in the apical meristem and the initial events of leaf morphogenesis.

Rapid high resolution fluorescent imaging of reporter gene activity

During our attempts to achieve cellular resolution of *RBCS* gene activity in the meristem, we investigated a variety of techniques for the visualization of GUS activity in small tissue samples. For this investigation, we used *RBCS* expression in leaf tissue as a standard, since there was

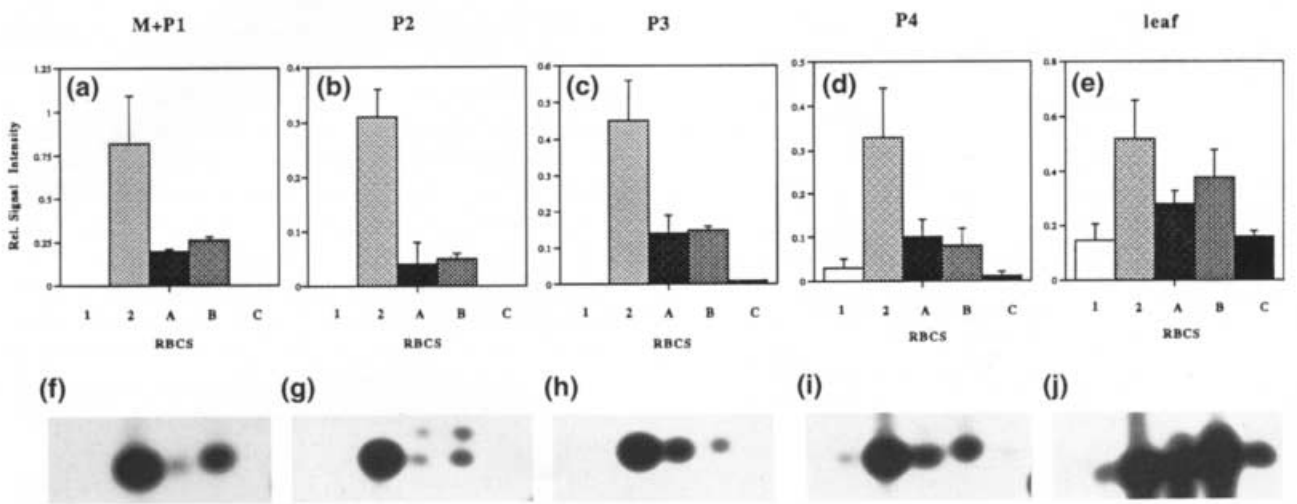

Figure 4. RT-PCR analysis of *RBCS* accumulation in developing primordia.
(a), (b), (c), (d) and (e) Bar charts obtained from RT-PCR analysis of primordia samples M+P1, P2, P3, P4 and leaf samples, respectively. The results have been expressed relative to the *RPL2* signals obtained from the same samples (error bars are standard deviation, n = 4).
(f), (g), (h), (i) and (j) Autoradiographs corresponding to typical samples used in the calculation of the results shown in the bar charts (a)–(e), respectively.

already literature on the expected expression pattern (e.g. Aoyagi *et al.*, 1988). Both the immunocytochemical and fluorescent imaging techniques yielded data on GUS expression under control of an *RBCS* 5′ sequence in line with those published on the *RBCS* transcript and protein. However, the embedded GUS histochemical assay revealed a low but definite signal in the leaf epidermis. Although there has been some debate in the literature on whether some photosynthetic genes are expressed in the epidermis (Dupree *et al.*, 1991), in our histochemical analyses we found it very difficult to discard the possibility of product diffusion either during the assay or during tissue preparation for analysis.

In contrast to the embedded histochemical and immunocytochemical assays, the fluorescent analysis provided a simple, rapid, reliable assay of GUS activity within the leaf. The tissue does not require fixation and remains in a viable state during the assay. In addition, computer processing of the digitilized image provides great flexibility in the analysis and storage of data. We find that the fluorescent analysis works well for the assay of highly active promoters (e.g. *RBCS*–GUS and 35S–GUS), but the analysis of weakly expressed promoters is more problemmatical (Fleming, unpublished data). The visualization of optical sections requires a high level of GUS activity in the tissue sample being examined, although computer-aided optimization of signal-to-noise ratio combined with the averaging of scans helps in the resolution of weaker signals. In addition, the analysis of tissue with relatively low autofluorescence (e.g. apical meristems) provides fewer problems with background noise than tissue with high autofluorescence (e.g. vascular tissue), although autofluorescence problems can be alleviated to some extent by the use of appropriate filters.

However, although the fluorescent imaging of GUS activity has a number of advantages over other methods of visualizing reporter gene activity, care must be taken in the interpretation of data obtained. The analysis reported here of *RBCS*–GUS activity in the apices of transgenic tomatoes provides an example of the utility of the fluorescent assay method.

RBCS *gene upstream elements are sufficient to mimic transcript accumulation patterns in the shoot apex*

With respect to the meristem, the results of our analysis indicate that 5′ sequences of the cloned *RBCS* genes were sufficient to reconstruct the pattern of transcript accumulation observed by *in situ* hybridization of *RBCS* in wild-type plants, that is, a relatively high signal in the developing leaf primordia and stem tissue, and virtually no signal in the meristem. By fluorescent imaging we could both rapidly analyse GUS activity in living tissue, and obtain good resolution of activity in some of the smallest cells in the plant. Such an analysis would not have been possible with other methods of GUS histochemistry.

In addition to the analysis of non-transgenic apices to account for the level of background fluorescence and substrate autocatalysis (Figure 2), we performed a number of controls. As a control for substrate accessibility into the meristem, we analysed transgenes containing the 35S–GUS construct, which we expected to provide a constitutive expression pattern (Benfey and Chua, 1990). Our results suggested a differential expression of the 35S promoter within the meristem (Figure 2c and d). However, analysis of acridine orange-stained apices also led to a similar pattern of signal (Figure 2e). Since analysis of thin sections

of the meristem either at the light or electron microscope level has not revealed any overt difference in nucleic acid distribution between the tunica and corpus layers (e.g. Fleming *et al.*, 1993; Lyndon and Robertson, 1976), we believe that the apparent difference in signal intensity observed with the 35S promoter may be a consequence of the parabolic shape of the intact meristem focussing light. Nevertheless, the fact that we can observe a fluorescent signal within the meristem using the 35S–GUS transgenes indicates that the lack of apparent signal in the *RBCS* transgenic apices reflects a lack of enzyme activity rather than any problem with substrate accessibility.

The pattern of *RBCS* expression revealed by fluorescent imaging is very similar to that observed by chlorophyll autofluorescence, suggesting a link between the two. The exception is the LI layer of the meristem. Neither by *in situ* hybridization analysis nor fluorescent imaging of promoter activity have we been able to detect *RBCS* expression in this layer, although a weak but definite autofluorescence is present (Figure 2h). From the previously described ultrastructure of the tomato apical meristem (Chandra Sekhar and Sawhney, 1985), the LI layer is distinct from the other cell layers in having electron dense bodies and partially differentiated plastids. Based on the barrier filters used, it is likely that the fluorescence we observe is due to chlorophyll, suggesting that these differentiating proplastids are synthesizing chlorophyll. At present, it is unclear why there should be chloroplast differentiation occurring in the LI layer but not in the other layers of the meristem, especially since the progeny of the LI cells (the epidermis) are characterized by having only a few fully developed chloroplasts (Dupree *et al.*, 1991).

RBCS *gene expression is developmentally controlled on leaf initiation*

Previous analysis has revealed that in addition to environmental signals, such as light, there is also a developmental aspect to the control of *RBCS* gene expression. This has been reported at the organ level (Kuhlemeier *et al.*, 1988; Wanner and Gruissem, 1991) as well as the tissue level (Langdale *et al.*, 1988), but generally using differentiated leaf tissue. In contrast, the results presented here obtained by imaging of reporter gene activity and RT-PCR provide an insight into the earliest events occurring during leaf development with respect to the photosynthetic machinery. The RT-PCR data suggest that there is an ordered activation of *RBCS* genes during the initial stages of leaf primordium development with transcripts for *RBCS2, RBCS3A* and *RBCS3B* detectable at all stages of primordium development and those for *RBCS1* and *RBCS3C* accumulating later. However, although we took great care to validate the RT-PCR assay (avoidance of primer competition in assays, verification of amplification linearity, probe hybridization to verify amplification product identity, amplification of similar sized products, and analysis of tissue samples shown by independent methods to have distinct patterns of *RBCS* transcript accumulation) caution is still needed in the comparison of values for transcript accumulation obtained using different primer sets (Dostal *et al.*, 1994; Wong *et al.*, 1994). Nevertheless, our data concur with the prevailing picture of a developmental component to *RBCS* gene expression in tomato, the functional significance of which remains unclear.

RBCS *gene expression in the apical meristem cannot be induced by light*

Our data indicate that *RBCS* promoter activity is absent from cells of the meristem, yet cells subtending the meristem (which are the 1- to 2-day-old progeny of cells in the meristem) express the *RBCS* genes to a high level. This raises the question of how such spatial regulation of transcript accumulation is achieved. Here we show that the meristem is non-responsive with respect to *RBCS* expression after exposure to light, an environmental signal which in other tissues has been shown to induce *RBCS* expression via a complex signal transduction pathway (Bowler and Chua, 1994). Although this analysis involved the dissection of the apex to reveal the meristem, it must be stressed that the meristem itself was not damaged and continued to function normally as assessed by the rate of leaf initiation. It is thus unlikely that the lack of induction of *RBCS* by light reflected a changed state of the tissue resulting from the dissection process. The non-expression of the *RBCS* transcripts in the apical meristem is more probably owing to a developmental repression of *RBCS* gene activity in this tissue which cannot be short circuited via light. Recently, both gene products (Chory, 1994) and signal transduction components leading from the light stimulus (Neuhaus *et al.*, 1993) have been identified which can effect *RBCS* gene expression. Our future work will be directed towards the manipulation of these identified modulators of *RBCS* gene expression to see whether any of them can alleviate the observed non-expression of *RBCS* in the apical meristem.

Experimental procedures

Plant material and tissue culture

For RT-PCR and *in situ* hybridization, seedlings of *Lycopersicon esculentum* cv. Moneymaker were grown in soil in a growth chamber at 22°C under a 16/8 h light regime until they had generated seven to eight leaves. For analysis of GUS expression by histochemical assay, immunocytochemistry and fluorescent imaging, transgenic F_1 seeds were germinated and grown under the same conditions described above.

The transgenic plants containing the tomato *RBCS* 5′ sequences

Table 2. Primers used in the RT-PCR analysis and PCR product size

Primer name and specificity	Sequence	PCR product
AF10 (body *RBCS*)	5′-AATGGATGGGTTCCTTGCTTGG-3′	–
AF21 (*RBCS1*, 3′)	5′-AAATCAAACAAACATTTTGATTATAT-3′	301 bp
AF22 (*RBCS2*, 3′)	5′-TGTCCCTAAAGACAATTTTGTTCC-3′	298 bp
AF23 (*RBCS3A*, 3′)	5′AACTGTCCCTATAAACATAGGGC-3′	307 bp
AF24 (*RBCS3B*, 3′)	5′-AGCTTGCCCTAAATACATAGCGT-3′	322 bp
AF25 (*RBCS3C*, 3′)	5′-GGAAAATGCAAACAGTTTCTCACT-3′	306 bp
AF40 (*RPL2*, 5′)	5′-GTGTCTTTGCTAGGTGTTCTGG-3′	–
AF41 (*RPL2*, 3′)	5′-GCCTTGGCTGCAGTAGCACG-3′	400 bp

were constructed as described by Meier *et al.* (1995). Briefly, the constructs used were translational fusions of the first 20 codons of each *RBCS* gene with GUS. In addition, the constructs contained approximately 3 kbp (*RBCS1*), 600 bp (*RBCS2*), 1 kbp (*RBCS3A*), 4 kbp (*RBCS3B*), or 2 kbp (*RBCS3C*) of the appropriate promoter. Constructs were terminated with the nos 3′ sequence. 35S–GUS transgenic seeds used were constructed either in the Gruissem laboratory or were the kind gift of Dr J. Jones (John Innes Centre, Norwich, UK).

For exposure of the apical meristem to light, apices of *RBCS*–GUS transgenic tomatoes were dissected to reveal the apical dome, leaving two primordia intact. The apices were cultured on a Murashige and Skoog medium (without hormones, with 1% (w/v) sucrose, 0.8 % (w/v) agar) under light for periods of up to 7 days. During this time the apices continued to grow and generate leaf primordia with a plastochron of approximately 2 days. Thin hand sections were then taken and the GUS activity in the apex visualized either by fluorescent imaging or X-Gluc histochemistry.

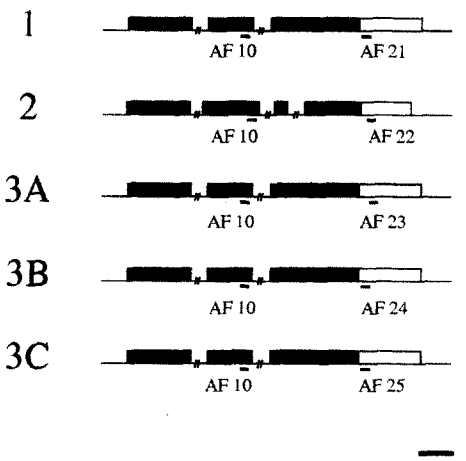

Figure 5. RT-PCR strategy for *RBCS* gene-specific amplification. Primers were selected based on the published sequences of the five RBCS genes in tomato (Sugita and Gruissem, 1987). A common 5′ primer in the coding region (AF10) was used with a gene-specific 3′ primer for each of the 3′ UTRs of the genes *RBCS1, RBCS2, RBCS3A, RBCS3B* and *RBCS3C* (AF21, AF22, AF23, AF24, AF25, respectively). The relative positions of the primers against the genomic sequences are shown and the sequences described in Table 2. Boxed region is the transcribed sequence; filled box is the translated region; open box is the untranslated region. Bar is 100 nt.

RT-PCR analysis

Apices of plants were dissected under a binocular microscope to yield four tissue samples, M+P1, P2, P3, and P4, as described in Table 1. RNA extraction was adapted from the method of Logemann *et al.* (1987). The tissue samples were collected immediately into the RNA extraction buffer (10 µl) at RT in a microfuge tube. After sufficient samples had been collected (10–15 tissue pieces for the smaller samples M+P1 and P2, seven to 10 pieces for the larger samples P3 and P4), the tissues were first physically squashed using sterile fine tweezers, as viewed under the binocular microscope through the wall of the microfuge tube. Samples were then briefly frozen in liquid nitrogen, thawed, then a further 40 µl of extraction buffer added containing 1 µg yeast tRNA as carrier. After mixing, the samples were vigorously vortexed with a mixture of phenol and chloroform, before being centrifuged at 12 000 ***g*** for 45 min at RT. Supernatants were then collected and precipitated overnight with 0.2 vol 1 M acetic acid and 0.7 vol ethanol. Precipitates were spun down at 4°C, then washed 2× at RT with 50 µl 3 M sodium acetate pH 5.2. Precipitates were finally washed in 50 µl 70% ethanol before being dried at RT. Samples were then taken up in 10 µl water and used directly for RT-PCR.

Reverse transcription was carried out under standard conditions using purchased buffer solution, dNTPs and AMV reverse transcriptase (Promega). The RNA samples were denatured before use by brief heating to 65°C and cooling on ice. Reverse transcription was performed at 42°C for 2 h. The enzyme was then heat inactivated, and the sample either used directly in the PCR reactions, or stored at –20°C.

PCR reactions were performed under standard conditions using purchased buffer, nucleotides and Taq polymerase (Promega). The cDNA reaction from each RNA sample was diluted in water

to provide a series of substrate concentrations over a 10 000-fold range (to assay for amplification linearity) which were added to the PCR reactions in a constant volume of 2 μl in a 50 μl reaction volume. Reactions were initiated using the hot start technique. Each *RBCS* transcript was amplified using a pair of primers in which one primer was constant for all amplifications (i.e. a body primer (AF10) in the conserved 3′ translated region of the published sequences) and a second primer (AF21-25) with specific binding to the 3′ UTR region of each *RBCS* transcript. The primer sequences used and the predicted amplification product sizes are listed in Table 2, and the binding sites shown in Figure 5. The primers were chosen using the published sequences (Sugita and Gruissem, 1987; Sugita *et al.*, 1987) and were selected so that the amplified sequences were of a similar size and crossed at least one intron boundary. PCR was performed in 50 μl volumes with an annealing temperature of 60°C (30 sec), extension at 71°C (30 sec) and denaturation at 94°C (30 sec) for 30 cycles. Final extension was performed at 71°C for 5 min.

Following amplification, 20 μl samples of PCR reaction products were run on 2% agarose gels, blotted on to nylon membranes, then hybridized at 60°C with a labelled DNA body probe for *RBCS* that bound to all amplified *RBCS* sequences. After washing to a final stringency of 0.1×SSC at 60°C for 10 min, an estimate of signal intensity for each sample was made by analysis of the blots on a phosphorimager (Bio-Rad) and hard copy data obtained by autoradiography using intensfying screens at -80°C. All *RBCS* hybridizations were performed using aliquots of the same labelled probe, and exposure time on the phosphorimager was for 2 h for all samples.

Fluorescent imaging of GUS activity

Samples were prepared by taking thin hand sections under a binocular microscope and incubating them directly in 0.5% (v/v) ImaGene Green (Molecular Probes, Oregon, USA) in 50 mM sodium phospate buffer (pH 7.2) in the dark at RT for 1–4 h. Samples were briefly washed in fresh buffer without substrate, then mounted under coverslips before analysis.

Analysis was performed using a Zeiss LSM microscope with excitation by an Argon 488 nm laser and viewing via a 515–560 nm barrier filter. Data were visualized by CCD and stored on optical discs. Initial data on signal expression were recorded using the microscope in non-confocal mode to provide an overall picture of GUS activity in whole tissues (fluorescent image). Fine analysis of activity was obtained by confocal microscopy using pinhole values of 20–25 and averaging of eight sequential scans. Scan speed was 1 sec. Pixel density 512×512. Contrast and brightness were adjusted to provide optimal resolution and signal contrast and signal intensity visualized using a glowscale. In all cases wild-type, non-transformed tissue was viewed in parallel using the same basic microscopy parameters to ensure that the signal observed in transgenic tissue reflected GUS activity rather than background fluorescence from either the tissue or autohydrolysis of the substrate. This latter problem only became significant during long incubations (6 h+).

For visualization of nucleic acids, hand sections were incubated in a 0.1% (w/v) solution of acridine orange before viewing using the same optical set up as for the GUS assay. For visualization of autofluorescence, tissue was excited with the 488 nm Argon laser and signal viewed via a 590 LP filter set.

Embedded GUS histochemical assay

Histochemical assays using X-Gluc were performed under standard conditions on thin hand sections of transgenic tissue (Jefferson *et al.*, 1987). After brief washing in 50 mM sodium phosphate buffer, samples were dehydrated through a series of ethanol solutions to 100% ethanol. After exchanging with xylene, samples were embedded in paraffin and thin sections (10 μm) cut on a microtome. Sections were mounted on slides, de-paraffinized in xylene, then mounted in Entellan.

Immunocytochemistry

Samples for immunocytochemistry were prepared as described for *in situ* hybridization (Fleming, 1995; Fleming *et al.*, 1993) except that an ethanol:acetic acid (1:1, v/v) fixative was used instead of formaldehyde/glutaraldehyde. Sections were hybridized with a polyclonal antibody against GUS (Clontech) and signal visualized by silver enhanced gold staining according to the manufacturer's instructions (Amersham).

Acknowledgements

We would like to thank Dr Hans Imboden (Neurobiology Institute, University of Berne) for introducing us to the confocal microscope, Kris Callan (Berkeley) for help in the production of the *RBCS*-GUS transgenic plants, and Cheryl Smart (ETH, Zürich) for critical reading of the manuscript. The research reported here was supported by grants from the Swiss National Science Foundation (C.K., A.J.F.) and the US National Science Foundation (W.G.).

References

Aoyagi, K., Kuhlemeier, C. and Chua, N.-H. (1988) The pea *RBCS3A* enhancer-like element directs cell-specific expression in transgenic tobacco. *Mol. Gen. Genet.* **213**, 179–185.

Benfey, P.N. and Chua, N.-H. (1990) The cauliflower mosaic virus 35S promoter: combinatorial regulation of transcription in plants. *Science,* **250**, 959–966.

Bowler, C. and Chua, N.H. (1994) Emerging themes of plant signal transduction. *Plant Cell,* **6**, 1529–1541.

Chandra Sekhar, K.N. and Sawhney, V.K. (1985) Ultrastructure of the shoot apex of tomato (*Lycopersicon esculentum*). *Am. J. Bot.* **72**, 1813–1822.

Chory, J. (1994) Plant phototransduction—phytochrome signal transduction. *Curr. Biol.* **4**, 844–846.

Dostal, D.E., Rothblum, K.N. and Baker, K.M. (1994) An improved method for absolute quantitation of mRNA using multiplex polymerase chain reaction: determination of renin and angiotensinogen mRNA levels in various tissues. *Anal. Biochem.* **223**, 239–250.

Dupree, P., Pwee, K.-H. and Gray, J.C. (1991) Expression of photosynthetic gene–promoter fusions in leaf epidermal cells of transgenic tobacco plants. *Plant J.* **1**, 115–120.

Fleming, A.J. (1995) Localization of RNA transcripts in plant tissue by *in situ* hybridization. In *Gene Transfer to Plants* (Potrykus, I. and Spangenberg, G., eds). Heidelberg: Springer Verlag, pp. 273–285.

Fleming, A.J. and Kuhlemeier, C. (1994) Activation of basal cells of the apical meristem during sepal formation in tomato. *Plant Cell,* **6**, 789–798.

Fleming, A.J., Mandel, T., Hofmann, S., Sterk, P., de Vries, S.C. and Kuhlemeier, C. (1992) Expression pattern of a tobacco lipid transfer protein gene within the shoot apex. *Plant J.* **2**, 855–862.

Fleming, A.J., Mandel, T., Roth, I. and Kuhlemeier, C. (1993) The patterns of gene expression in the tomato shoot apical meristem. *Plant Cell,* **5**, 297–309.

Jefferson, R.A., Kavanagh, T.A. and Bevan, M.W. (1987) GUS fusions: β-glucoronidase as a sensitive and versatile gene fusion marker in higher plants. *EMBO J.* **6**, 3901–3907.

Kuhlemeier, C., Cuozzo, M., Green, P.J., Goyvaerts, E., Ward, K. and Chua, N.-H. (1988) Localization and conditional redundancy of regulatory element in *RBCS3A*, a pea gene encoding the small subunit of ribulose-bisphosphate carboxylase. *Proc. Natl Acad. Sci.* **85**, 4662–4666.

Langdale, J.A., Rothermel, B.A. and Nelson, T. (1988) Cellular pattern of photosynthetic gene expression in developing maize leaves. *Genes Devel.* **2**, 106–115.

Logemann, J., Schell, J. and Willmitzer, L. (1987) Improved method for the isolation of RNA from plant tissues. *Anal. Biochem.* **163**, 16–20.

Lyndon, R.F. and Robertson, E.S. (1976) The quantitative ultrastructure of the pea shoot apex in relation to leaf initiation. *Protoplasma,* **87**, 387–402.

Meier, I., Callan, K.L., Fleming, A.J. and Gruissem, W. (1995) Organ-specific differential regulation of a promoter subfamily for the ribulose-1, 5-bisphosphate carboxylase/oxygenase small subunit genes in tomato. *Plant Physiol.* **107**, 1105–1118.

Neuhaus, G., Bowler, C., Kern, R. and Chua, N.-H. (1993) Calcium/calmodulin-dependent and -independent phytochrome signal transduction pathways. *Cell,* **73**, 937–952.

Sugita, M. and Gruissem, W. (1987) Developmental, organ-specific, and light dependent expression of the tomato ribulose-1,5- bisphosphate carboxylase small subunit gene family. *Proc. Natl Acad. Sci. USA,* **84**, 7104–7108.

Sugita, M., Manzara, T., Pichersky, E., Cashmore, A. and Gruissem, W. (1987) Genomic organization, sequence analysis and expression of all five genes encoding the small subunit of ribulose-1,5-bisphosphate carboxylase/oxygenase from tomato. *Mol. Gen. Genet.* **209**, 247–256.

Wanner, L.A. and Gruissem, W. (1991) Developmental, organ-specific, and light dependent expression of the tomato ribulose-1, 5-bisphosphate carboxylase small subunit gene family. *Proc. Natl Acad. Sci. USA,* **84**, 7104–7108.

Wong, H., Anderson, W.D., Cheng, T. and Riabowol, K.T. (1994) Monitoring mRNA expression by polymerase chain reaction: the 'primer-dropping' method. *Anal. Biochem.* **223**, 251–258.